Compact Coplanar Waveguide (CPW)-Fed Zeroth-Order Resonant Antennas With Extended Bandwidth and High Efficiency on Vialess Single Layer

Taehee Jang, *Student Member, IEEE*, Jaehyurk Choi, and Sungjoon Lim, *Member, IEEE*

***Abstract*—This paper presents the design and analysis of compact coplanar waveguide (CPW)-fed zeroth-order resonant (ZOR) antennas. They are designed on a CPW single layer where vias are not required. The ZOR phenomenon is employed to reduce the antenna size. The novel composite right/left-handed (CRLH) unit cell on a vialess single layer simplifies the fabrication process. In addition, the CPW geometry provides high design freedom, so that bandwidth-extended ZOR antennas can be designed. The antenna's bandwidth is characterized by the circuit parameters. Based on the proposed bandwidth extension technique, symmetric, asymmetric, and chip-loaded antennas are designed. The ZOR characteristic and bandwidth extension are verified by a commercial EM simulator. Their performances are compared with those of previously reported metamaterial resonant antennas. They provide further size reduction, higher efficiency, easier manufacturing, and extended bandwidth.**

***Index Terms*—Co-planar waveguide (CPW), composite right/left-handed transmission line, metamaterials, small antenna.**

I. Introduction

METAMATERIALS have been widely studied for microwave circuit and antenna applications [1]–[7]. They have unique properties in comparison with conventional nature materials, such as anti-parallel phase and group velocities, and a zero propagation constant [1]–[5] and can be realized by means of split-ring resonators (SRRs) or composite right/left-handed (CRLH) transmission lines (TLs). Especially, the CRLH TL is able to easily achieve left-handed (LH) metamaterial properties by way of the circuit parameters [6]. By using the features of the anti-parallel phase and group velocities, CRLH TLs can be applied to dominant mode leaky-wave antennas radiating in the backward and forward directions [7]. In addition, due to the zero propagation constant inherent in the LH metamaterial properties, the resonator has an infinite wavelength and its resonant frequency is independent of the size of the resonator. Therefore, the zero propagation constant properties of resonant antennas enable them to be more compact than conventional half-wavelength antennas [8]–[10]. Although they offer the advantage of size reduction, it is difficult to apply them to modern wireless communication systems because of their narrow bandwidth.

Recently, many researchers have attempted to solve the bandwidth problem of zeroth-order resonant (ZOR) antennas [11]–[15]. To accomplish this, a metamaterial ring antenna was reported in [11]. This antenna was implemented on a multi-layer structure in which a thick substrate with low permittivity is additionally employed. The substrate is supported by holding brackets and its bandwidth is increased up to 6.8% by means of a sleeve balun. Alternatively, the bandwidth of the ZOR antenna is increased by a strip matching ground [12]. In this case, the fractional bandwidth of the antenna was enhanced by up to 8%. It is also built on multiple substrates where a thin substrate with high permittivity is stacked on a thick substrate with low permittivity. The other method is to have two resonant frequencies close to each other [13]. Such an antenna consists of two resonators whose resonant frequencies are slightly different. The bandwidth is increased by up to 3.1%.

This paper presents novel compact coplanar waveguide (CPW)-fed zeroth-order resonant antennas. Three types of antennas are proposed whose bandwidths are extended by up to 8.9% and they are built on a single layer without a via process. The size of the proposed antenna can be reduced, due to their infinite wavelength, while keeping a high radiation efficiency. According to [6], the Q-factor of the ZOR mode is determined by the shunt inductance and capacitance. In other words, the antenna's bandwidth can be increased by manipulating its shunt reactance. Especially, since a CPW structure gives a lot of design freedom, it provides the benefits of easy design to implement the desired circuit parameters. Moreover, the use of a via free and single layer process results in a simpler fabrication process compared with that of the broad metamaterial resonant antennas proposed in [10]–[12].

This paper is organized as follows. Sections II and III demonstrate the principle of the CPW-based ZOR antenna and the bandwidth extension through the design parameters rather than the material properties. The input impedance, internal energy,

Manuscript received March 11, 2010; revised June 10, 2010; accepted July 07, 2010. Date of publication December 03, 2010; date of current version February 02, 2011. This work was supported in part by the IT R&D program of MKE/KEIT [KI002084, A Study on Mobile Communication Systems for Next-Generation Vehicles with Internal Antenna Array] and in part by the National Research Foundation of Korea Grant funded by the Korean Government [2009-0071958].

The authors are with the School of Electrical and Electronics Engineering, College of Engineering, Chung-Ang University, Seoul, Korea (e-mail: sungjoon@cau.ac.kr).

Color versions of one or more of the figures in this paper are available online at http://ieeexplore.ieee.org.

Digital Object Identifier 10.1109/TAP.2010.2096191

0018-926X/$26.00 © 2010 IEEE

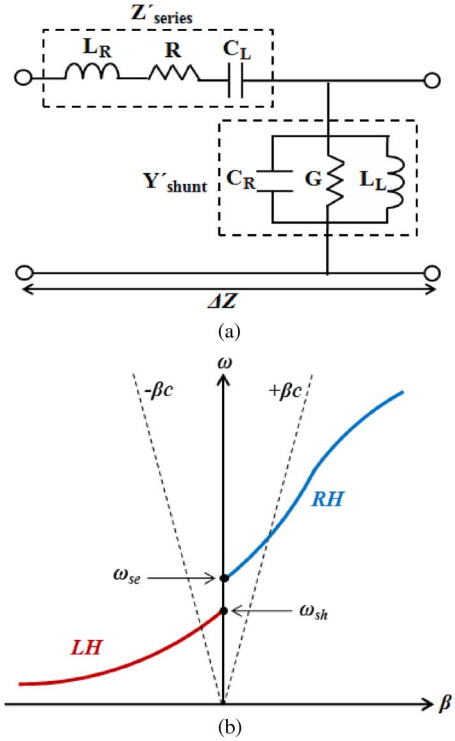

Fig. 1. Illustration of (a) equivalent circuit model of the CRLH unit cell and (b) its dispersion curve.

and quality (Q) factor are analyzed. In this paper, three antenna configurations are presented employing the proposed idea. The three antennas, viz. symmetric, asymmetric, and chip inductor-loaded antennas, are proposed in Section IV. In Section V, their performances are compared with those of previously reported metamaterial resonant antennas. Finally, our conclusions are drawn in Section VI.

II. ZOR Antenna Theory

As shown in Fig. 1, a general CRLH TL is composed of series capacitance (C_L) and inductance (L_R) as well as a shunt capacitance (C_R) and inductance (L_L) [1]. It is designed in a periodic configuration by cascading N unit cells. The immittances of a lossy CRLH TL are given by

$$Z'_{series} = R + j\left(\omega L_R - \frac{1}{\omega C_L}\right) \tag{1}$$

$$Y'_{shunt} = G + j\left(\omega C_R - \frac{1}{\omega L_L}\right) \tag{2}$$

where R and G are the series resistance and shunt conductance of the lossy CRLH TL, respectively [17], [20]. The series and shunt resonant frequencies are given by

$$\omega_{se} = \frac{1}{\sqrt{L_R C_L}} \quad \text{rad/s} \tag{3}$$

$$\omega_{sh} = \frac{1}{\sqrt{L_L C_R}} \quad \text{rad/s}. \tag{4}$$

Thus, the complex propagation constant (γ) and characteristic impedance (Z_C) are

$$\gamma = \alpha + j\beta = \sqrt{Z'_{series} Y'_{shunt}} \tag{5}$$

$$Z_C = \sqrt{\frac{Z'_{series}}{Y'_{shunt}}} = \sqrt{\frac{L_L}{C_L}} \sqrt{\frac{(\omega/\omega_{se})^2 - 1}{(\omega/\omega_{sh})^2 - 1}}. \tag{6}$$

Because the CRLH TLs have periodic boundary conditions, the Bloch-Floquet theorem can be applied and its dispersion relation is determined by

$$\beta(\omega) = \frac{s(\omega)}{\Delta Z} \sqrt{\omega^2 L_R C_R + \frac{1}{\omega^2 L_L C_L} - \frac{L_R C_L + L_L C_R}{L_L C_L}} \tag{7}$$

where $s(\omega)$ and ΔZ are a sign function and the differential length, respectively.

For instance, ω_{se} and ω_{sh} can be unequal in the dispersion diagram of the unbalanced LC-based CRLH TL as shown in Fig. 1(b). At these resonant frequencies, where $\beta = 0$, an infinite wavelength can be supported. According to the theory of the open-ended resonator with the CRLH TL [6], its resonance occurs when

$$\beta_n = \frac{n\pi}{l} \, (n = 0, \pm 1, \ldots, \pm(N-1)) \tag{8}$$

where l, n and N are the physical length of the resonator, mode number, and number of unit cells, respectively. When n is zero, the wavelength becomes infinite and the resonant frequency of the zeroth-order mode becomes independent of the size of the antenna, while the shortest length of the conventional open-ended resonator is one half of the wavelength. Thus, an antenna with a more compact size can be realized.

As depicted in Fig. 1(b), for the unbalanced CRLH TL, two resonant frequencies, ω_{se} and ω_{sh}, with $\beta = 0$ are observed with a matched load. Considering the open-ended TL, where $Z_L = \infty$, the input impedance (Z_{in}) seen from one end of the resonator toward the other end is given by

$$\begin{aligned} Z_{in}^{open} &= -jZ_c \cot(\beta\ell) \overset{\beta \to 0}{\approx} -jZ_c \frac{1}{\beta\ell} \\ &= -j\sqrt{\frac{Z'_{series}}{Y'_{shunt}}} \left(\frac{1}{-j\sqrt{Z'_{series} Y'_{shunt}}}\right) \frac{1}{\ell} = \frac{1}{Y'_{shunt}\ell} \\ &= \frac{1}{Y'_{shunt}(N\Delta z)} \end{aligned} \tag{9}$$

where Y'_{shunt} is the admittance of the CRLH unit cell.

Since, from (9), the input impedance of the open-ended resonator is equal to $1/N$ times $1/Y'_{shunt}$ of the unit cell, the equivalent L, C, G values are equal to L_L/N, NC_R, and $1/NG$, respectively [18]. Regardless of N, the resonant frequency of the N cascaded open-ended ZOR circuit is determined by the resonant frequency originating from the shunt LC tank (Y'_{shunt}). Thus, the open ended ZOR antenna's resonant

frequency is given by (4), so that it depends only on the shunt parameters of the unit cell.

III. Proposed Bandwidth Extension Technique

A. Bandwidth Extension of ZOR Antenna

Considering that the open ended resonator is only dependent on Y'_{shunt} of the unit cell, the average electric energy stored in the shunt capacitor, C_R, is given by

$$W_e = \frac{1}{4}|V^2|NC_R \tag{10}$$

and the average magnetic energy stored in the shunt inductor, L_L, is

$$W_m = \frac{1}{4}|I_L|^2\frac{L_L}{N} = \frac{1}{4}|V|^2\frac{N}{\omega^2 L_L} \tag{11}$$

where I_L is the current through the inductor.

Because resonance occurs when W_m is equal to W_e, the quality factor can be calculated as follows:

$$\begin{aligned} Q &= \omega\frac{(average\ energy\ stored)}{(energy\ loss/\text{second})} \\ &= \omega_{sh}\frac{2W_m}{P_{loss}} = \frac{1/NG}{\omega_{sh}(L_L/N)} = \frac{1/G}{\omega_{sh}L_L} \\ &= \omega_{sh}(1/NG)\cdot NC_R = \omega_{sh}(1/G)C_R \\ &= \frac{1}{G}\sqrt{\frac{C_R}{L_L}}. \end{aligned} \tag{12}$$

Therefore, in the open ended case, the fractional bandwidth of the resonator is given by

$$BW = G \times \sqrt{\frac{L_L}{C_R}}. \tag{13}$$

Although this equation does not consider the impedance matching at the input terminals, it provides an intuitive concept by means of which the bandwidth can be efficiently increased.

Generally, ZOR antennas are known to have a narrow bandwidth problem compared to conventional resonant antennas. This is because the Q-factor of a ZOR antenna is only related to C_R and L_L. For example, in a microstrip structure, L_L and C_R are realized by the shorting pin (via) and parallel plate between the top patch and bottom ground. Since L_L in a microstrip line (MSL) depends on the length of the via, the microstrip structure limits the value of L_L. In addition, since the thickness and size of the substrate determine the capacitance of the parallel plate, the MSL has a large C_R. According to (13), the narrow bandwidth is originated from the small L_L and large C_R. Therefore, the ZOR antenna in microstrip technology has a narrow bandwidth due to the structural problem. In order to extend the bandwidth of the microstrip structure, a thick substrate with low permittivity is generally utilized. However, this causes fabrication difficulties and reduces the design freedom.

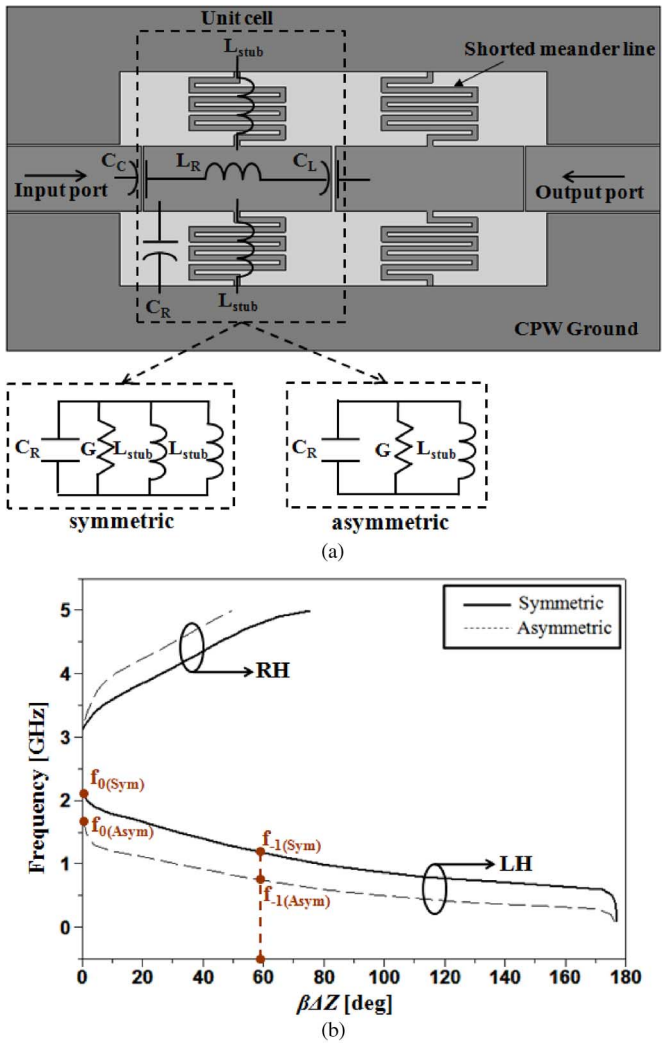

Fig. 2. Configuration of the proposed CRLH TL based on the CPW structure. (a) Unit cell design. (b) Dispersion diagram of symmetric and asymmetric unit cells.

In this paper, we focus on antennas with a large L_L and small C_R, which result in improved bandwidth without degrading the efficiency, due to the shunt conductance (G). Moreover, we suggest a structure which can be easily fabricated and offers more design freedom. Fig. 2(a) shows the proposed unit cell of the CPW-type CRLH TL. Through the parameter extraction of the proposed unit cell [20], the physical dimensions shown in Fig. 3 are determined. Based on the extracted parameters and (7), the dispersion diagrams for the symmetric and asymmetric unit cells are presented in Fig. 2(b). In addition, the values of the circuit parameters $(\mathrm{L_L}, \mathrm{C_R}, \mathrm{L_R}, \mathrm{C_L})$ are extracted from the s-parameter results. The shunt parameters of the proposed CPW-type structure are obtained from the shunt capacitance between the top patch and CPW ground, and the shunt inductance of the shorted meander lines. When the unit cell is realized in the symmetric configuration, the total shunt inductance, L_L, is equal to one half of the inductance of the meander line. This is because the two meander lines are connected in parallel $(L_L = L_{stub}/2)$. Since this CPW TL provides more design freedom for the reactive parameters compared with the MSL,

both a wider bandwidth and smaller size can be achieved by using a proper design. Therefore, the meander lines facilitate the realization of a short stub, as well as a large total L_L. Because the top patch is positioned far from the CPW ground, C_R is smaller than that of the microstrip structure, which also enables the bandwidth to be extended.

The inductance can be increased in proportion to the length of the shorted stub line. Therefore, the meander line enables a large L_L to be realized in a limited space. In addition, the signal and ground planes are placed on the co-plane so that the shunt capacitance between the top patch and CPW ground patch can be easily adjusted. Thus, the CPW technology and meander lines provide a means of changing the shunt parameters very easily.

In addition, in order to match the impedance, a stub on the top of the substrate and a partial bottom patch are also utilized. Both the width and length of the stub on the top play important roles in impedance matching. The bottom patch is placed under the top patch. Moreover, the bottom patch can be placed under the top patch to match the impedance. From Fig. 4(a), the larger overlapping area of $(L_3 \times W_3)$ and $(L_1 \times W_2)$ results in higher coupling capacitance (C_C) in the feed network. In addition, when the size of the bottom ground patch $(L_3 \times W_3)$ is increased as shown in Fig. 4(b), the value of C_R is increased. Therefore, good impedance matching can be obtained by adjusting the size and position of the bottom ground.

IV. Antenna Realization

In this section, the three configurations of zeroth-order antennas are realized. Each antenna has two unit cells and their resonant frequencies are determined by the shunt parameters.

A. Symmetric & Asymmetric Antenna Design

The proposed CPW based ZOR metamaterial antennas are illustrated in Fig. 3. They are composed of top metallic patches, shorted meander lines, a CPW ground plane, and bottom patch. The proposed ZOR antennas are realized by cascading the CPW-type unit cell periodically. In order to realize the L_L, the meander lines are connected between the top patch and the CPW grounds as the shorted stub. Fig. 3(a) shows the configuration of the symmetric antenna. The meander lines of the ZOR antenna are symmetrically aligned on both sides of the CPW GND. The bottom patch is placed under the top patch for the sake of impedance matching. In order to further reduce the resonant frequency of the antenna without changing the size, one side of the meander lines is removed, as shown in Fig. 3(b). Therefore, the meander lines in the unit cell are asymmetrically placed on only one side of the CPW GND.

Since the shorted meander lines are connected in parallel, the shunt inductance of the antenna is approximately twice that of the symmetric case. Thus, the resonant frequencies of the symmetric and asymmetric antennas are given by

$$\omega_{sh-sym} = \frac{1}{\sqrt{(L_{stub}||L_{stub})C_R}} = \frac{\sqrt{2}}{\sqrt{L_{stub}C_R}} = \sqrt{2} \times \omega_{sh-asym} \quad [\text{rad/s}] \tag{14}$$

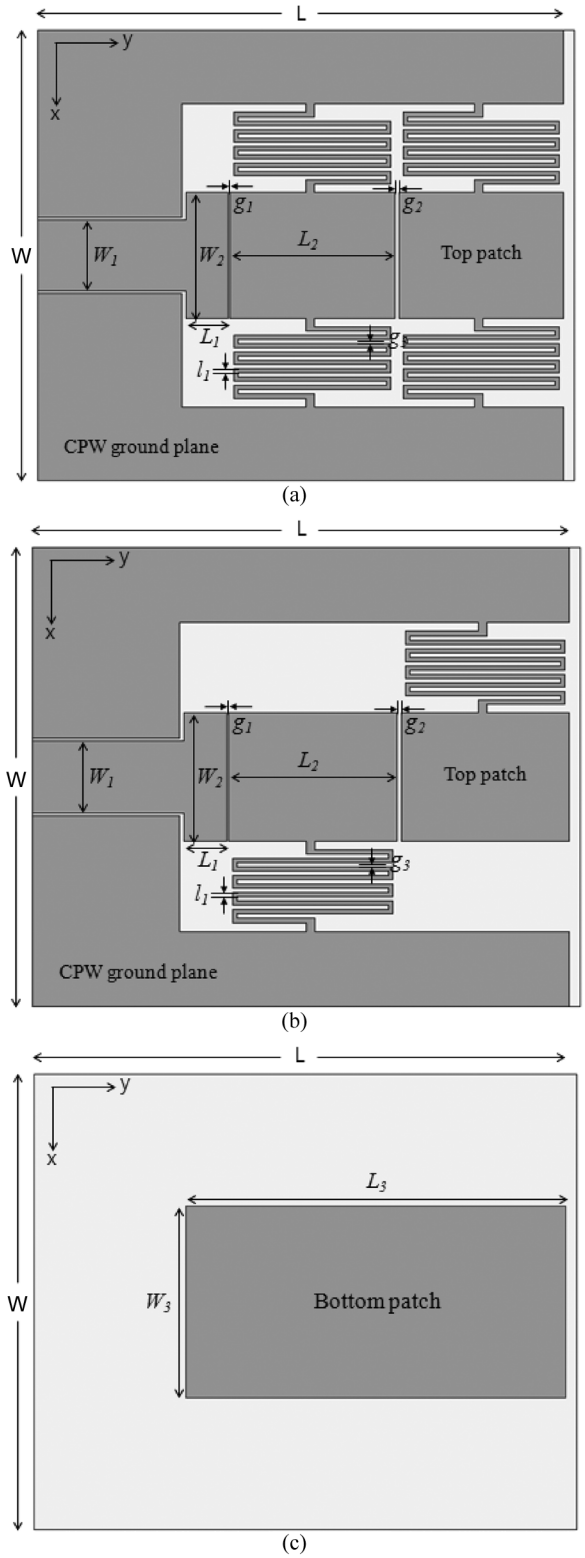

Fig. 3. Configuration of the proposed CPW-type ZOR antenna. (a) Top of symmetric unit cell. (b) Top of asymmetric unit cell. (c) Bottom of symmetric and asymmetric unit cells.

$$\omega_{sh-asym} = \frac{1}{\sqrt{L_{stub}C_R}} \quad [\text{rad/s}] \tag{15}$$

where L_{stub} is the inductance of the shorted meander line, and ω_{sh-sym} and $\omega_{sh-asym}$ are the resonant frequencies of the symmetric and asymmetric antenna, respectively.

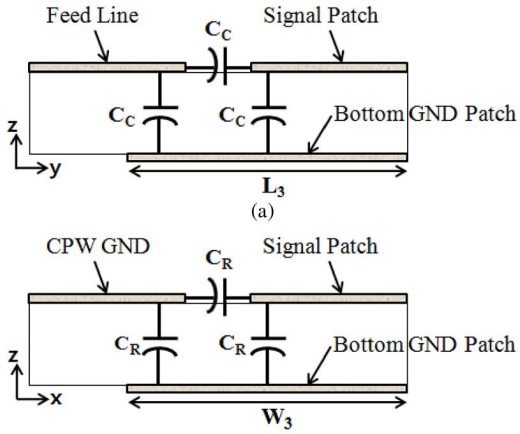

Fig. 4. Schematic explanation for the function of the bottom patch (a) the relationship between L_3 and C_C (b) the relationship between W_3 and C_R.

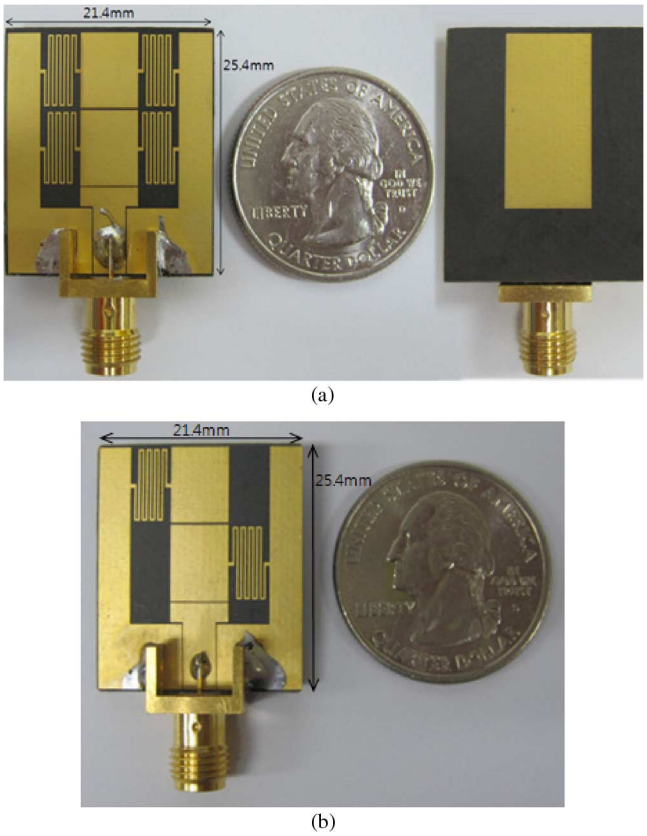

Fig. 5. Prototype of (a) top and bottom view of the symmetric antenna, (b) top view of the asymmetric antenna.

B. Symmetric & Asymmetric Antenna Performance

The proposed ZOR antennas are fabricated on Rogers RT/ Duroid 5880 substrates with a dielectric constant of 2.2 and thickness of 1.6 mm. A CPW feeding line of 50 Ω and proximity coupling are used as the feed network so that the input impedance is matched to 50 Ω. The resonant frequency of the proposed antenna is determined by L_{stub} and C_R between the top patch and CPW ground. By changing the length of the meander line, the L_L is changed so that the resonant frequency is altered. These antennas are built in the CPW configuration and printed on the top and bottom of a substrate without vias. Thus,

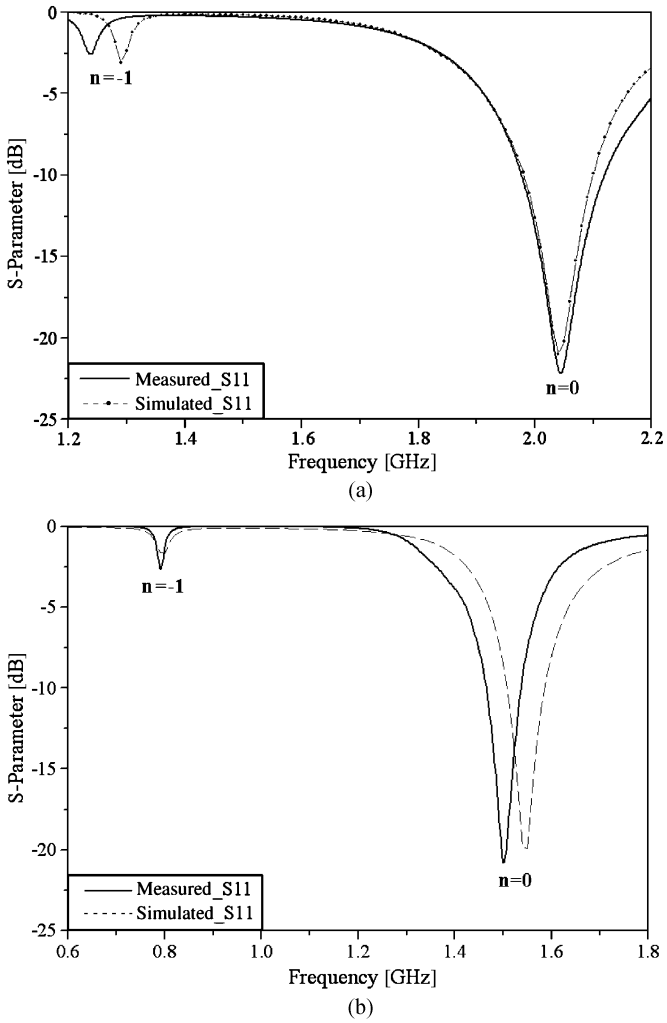

Fig. 6. Simulated and measured reflection coefficients of the proposed CPW-type ZOR antennas: (a) symmetric antenna, (b) asymmetric antenna.

the proposed antennas provide the features of easy fabrication and low profile configuration.

The symmetric antenna's dimensions are (unit: millimeter): $L_1 = 2$, $L_2 = 7.8$, $L_3 = 17.8$, $W_1 = 3.4$, $W_2 = 6$, $W_3 = 9$, $g_1 = 0.1$, $g_2 = g_3 = 0.2$, $l_1 = 0.2$ as shown in Fig. 3(a). With these dimensions, the extracted values for the unit cell consist of a C_R of 0.62 pF, L_L of 9.26 nH, and G of 0.0007. The fabricated prototype is shown in Fig. 5(a). The proposed antenna is designed to have its zeroth-order mode at 2.03 GHz. The electrical size of the unit cell of the antenna is $0.097\lambda_0 \times 0.053\lambda_0$ at 2.03 GHz. The overall area of the radiating aperture is approximately $0.145\lambda_0 \times 0.172\lambda_0 \times 0.011\lambda_0$ (21.4 mm $\times$ 25.4 mm $\times$ 1.6 mm). Fig. 6(a) shows the simulated and measured reflection coefficients where both resonant frequencies of the zeroth-order mode are 2.03 GHz. Moreover, the measured 10 dB bandwidth and radiation efficiency are 6.8% and 62%, respectively. Fig. 7 shows the simulated and measured radiation patterns on the Y-Z (E-plane) and X-Z (H-plane) planes at 2.03 GHz. Figs. 7(a) and (b) show the electric field distribution of the symmetric ZOR antenna in the $n = -1$ and $n = 0$ modes, respectively. The electric field distribution of the $n = -1$ mode is 180° out of phase along the aperture. As shown in Fig. 8(b), the electric field distribution for the $n = 0$ is in-phase.

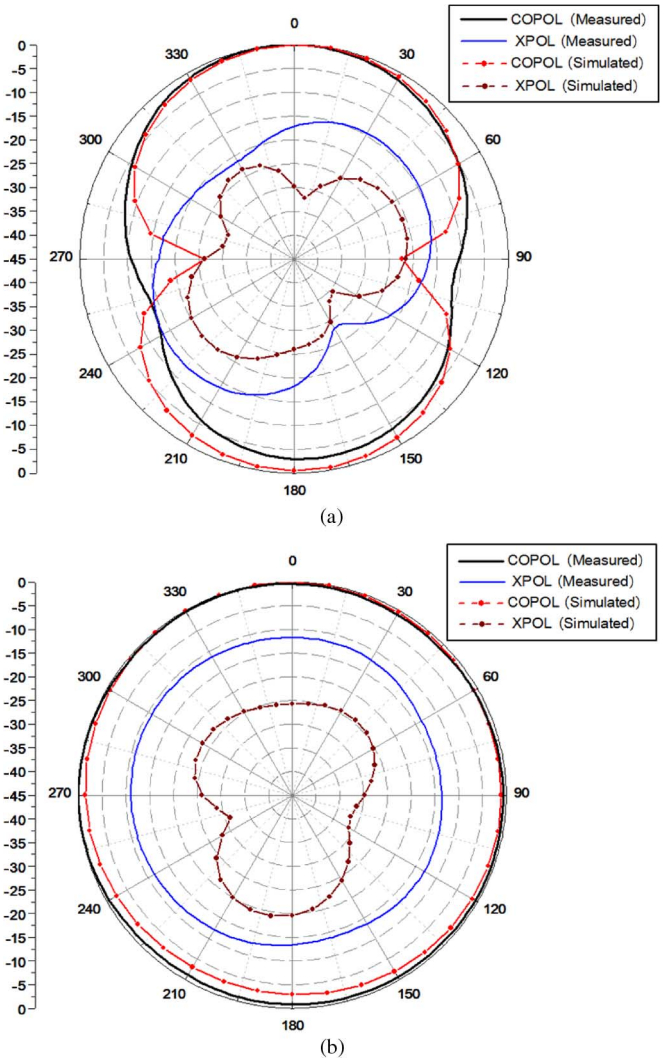

Fig. 7. Simulated and measured radiation patterns of the symmetric antenna at 2.03 GHz: (a) y-z plane (E-plane), (b) x-z plane (H-plane).

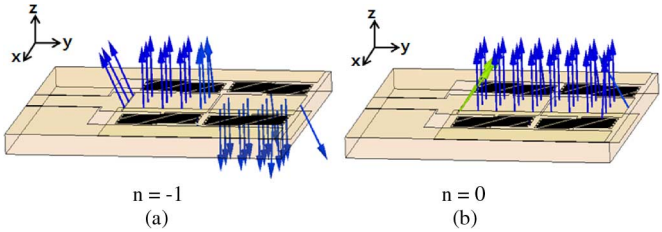

Fig. 8. Electric-field distribution of the symmetric antenna: (a) $n = -1$ mode, (b) $n = 0$ mode.

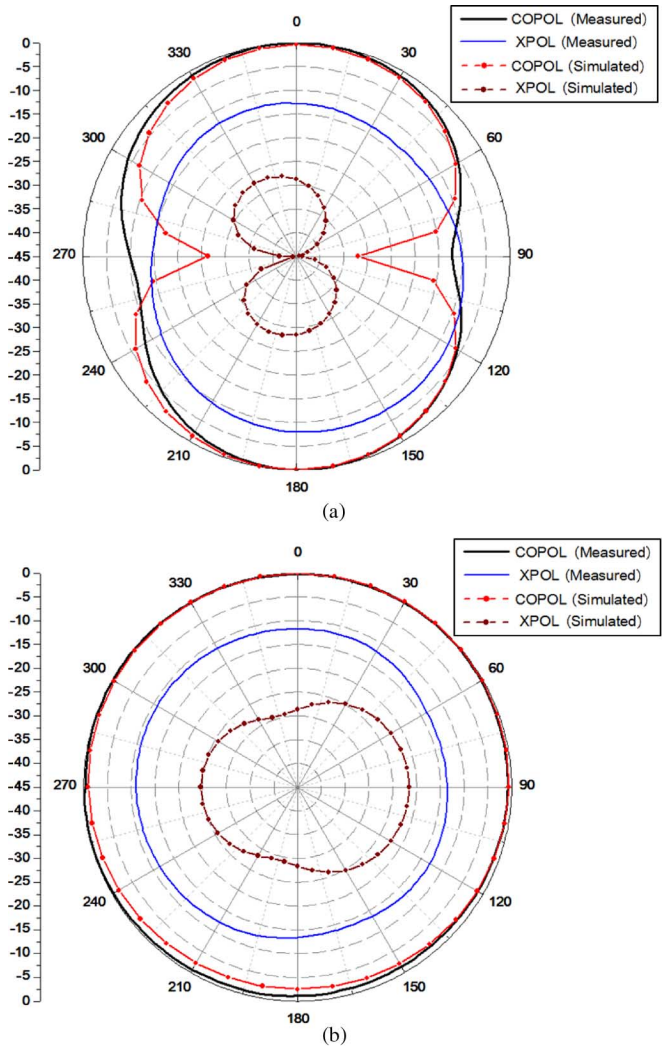

Fig. 9. Simulated and measured radiation patterns of the asymmetric antenna at 1.5 GHz (a) y-z plane (E-plane), (b) x-z plane (H-plane).

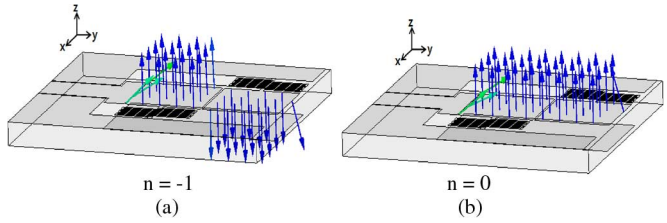

Fig. 10. Electric-field distribution of the asymmetric ZOR antenna (a) $n = -1$ mode and (b) $n = 0$ mode.

The asymmetric configuration can be implemented with a single meander line in each unit cell, while the symmetric one has two meander lines. Its dimensions are (unit: millimeter): $L_1 = 2$, $L_2 = 7.8$, $L_3 = 17.8$, $W_1 = 3.4$, $W_2 = 6$, $W_3 = 9$, $g_1 = 0.1$, $g_2 = g_3 = 0.2$, $l_1 = 0.2$. The fabricated prototype is shown in Fig. 5(b). It is designed to have the zeroth-order mode at 1.5 GHz. The electrical size of the unit cell of the antenna is $0.072\lambda_0 \times 0.04\lambda_0$ at 1.5 GHz. The overall area of the radiating patch is approximately $0.107\lambda_0 \times 0.127\lambda_0 \times 0.008\lambda_0$ ($21.4\,\text{mm} \times 25.4\,\text{mm} \times 1.6\,\text{mm}$). In Fig. 6(b), the simulated and measured reflection coefficients are shown, where the resonant frequency of the zeroth-order mode is observed to be 1.5 GHz and the 10 dB bandwidth is 4.8%. Figs. 9(a) and (b) show the simulated and measured radiation patterns on the Y-Z (E-plane) and X-Z (H-plane) planes at 1.5 GHz, respectively. The measured radiation efficiency is 42.5%. As shown in Fig. 10(a), the electric field distribution in the $n = -1$ mode is 180° out of phase. Fig. 10(b) shows that the electric field distribution is in-phase at $n = 0$.

The overall antenna performances of the proposed antennas are compared with those of the previously reported ZOR antennas [10]–[12] in Table I. Although the proposed antennas are

TABLE I
ANTENNA MEASUREMENT SUMMARY AND COMPARISON RESULTS OF PROPOSED AND REFERENCE ANTENNAS

	This Work (Symmetric)	This Work (Asymmetric)	[10]	[11]	[12]
Frequency (GHz)	2.03	1.5	3.38	1.77	1.73
Size (λ_0)	$0.097 \times 0.053 \times 0.011$	$0.072 \times 0.04 \times 0.008$	$0.16 \times 0.08 \times 0.011$	$0.09 \times 0.077 \times 0.036$	$0.1 \times 0.1 \times 0.015$
Bandwidth (%)	6.8	4.8	~0.1	6.8	8
Efficiency (%)	62	42.5	70	54	-
Via Process	Not required	Not required	Required	Required	Required
Layer	Single	Single	Single	Multi	Multi

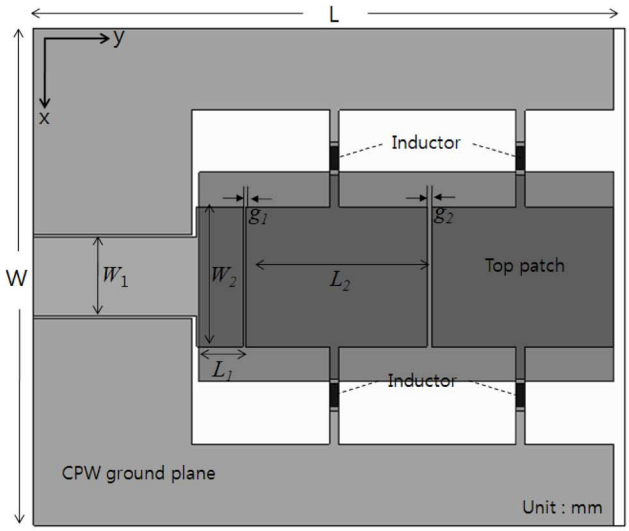

(a)

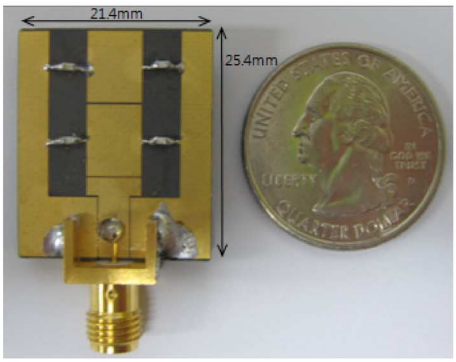

(b)

Fig. 11. (a) Configuration of the proposed chip-loaded ZOR antenna, (b) Top view of the fabricated prototype.

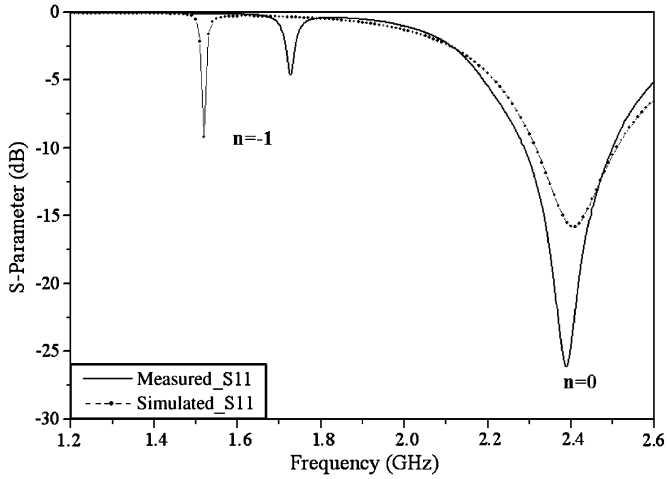

Fig. 12. Simulated and measured reflection coefficients of the chip-loaded ZOR antenna.

realized on a single layer without vias, they provide competitively enhanced bandwidths and high efficiencies. Moreover, they are smaller size than the conventional ZOR antenna [10] and are easy to fabricate owing to the vialess single layer.

C. Chip-Loaded Zeroth-Order Antenna

The configuration and prototype of the proposed chip-loaded antenna are shown in Fig. 11. The chip-loaded antenna is designed with lumped elements (chip inductor) instead of shorted stubs. Because this antenna is able to have a high shunt inductance, it is suitable for low frequency applications.

It is realized with high frequency chip inductors having an inductance of 8.2 nH. This antenna has a zeroth-order resonant frequency at $f_0 = 2.38$ GHz. The measured radiation efficiency at $f_0 = 2.38$ GHz was approximately 77.8%. The proposed chip-loaded antenna is fabricated on a Rogers RT/Duroid 5880 substrate with a dielectric constant of 2.2 and thickness of 1.6 mm as well. Its dimensions are (unit: millimeter): $L_1 = 2$, $L_2 = 7.8$, $L_3 = 17.8$, $W_1 = 3.4$, $W_2 = 6$, $W_3 = 9$, $g_1 = 0.1$, $g_2 = 0.2$.

It is also built with a CPW configuration and the shorted meander lines are replaced by the chip inductors. Thus, the resonant frequency can be tuned by changing the inductance values. The electrical size of the unit cell of the antenna is $0.128\lambda_0 \times 0.07\lambda_0$ at 2.38 GHz. The overall area of the antenna is approximately $0.170\lambda_0 \times 0.201\lambda_0 \times 0.012\lambda_0$ $(21.4\,\text{mm} \times 25.4\,\text{mm} \times 1.6\,\text{mm})$. The simulated and measured reflection coefficients are shown in Fig. 12. The reflection coefficient is lower than -10 dB over the entire frequency range of 2.29–2.50 GHz so that a 10 dB bandwidth of 8.9% is achieved. Fig. 13 shows the measured and simulated radiation patterns on the Y-Z (E-plane) and X-Z (H-plane) planes at 2.38 GHz. The cross-polarization was lower than -11 dB.

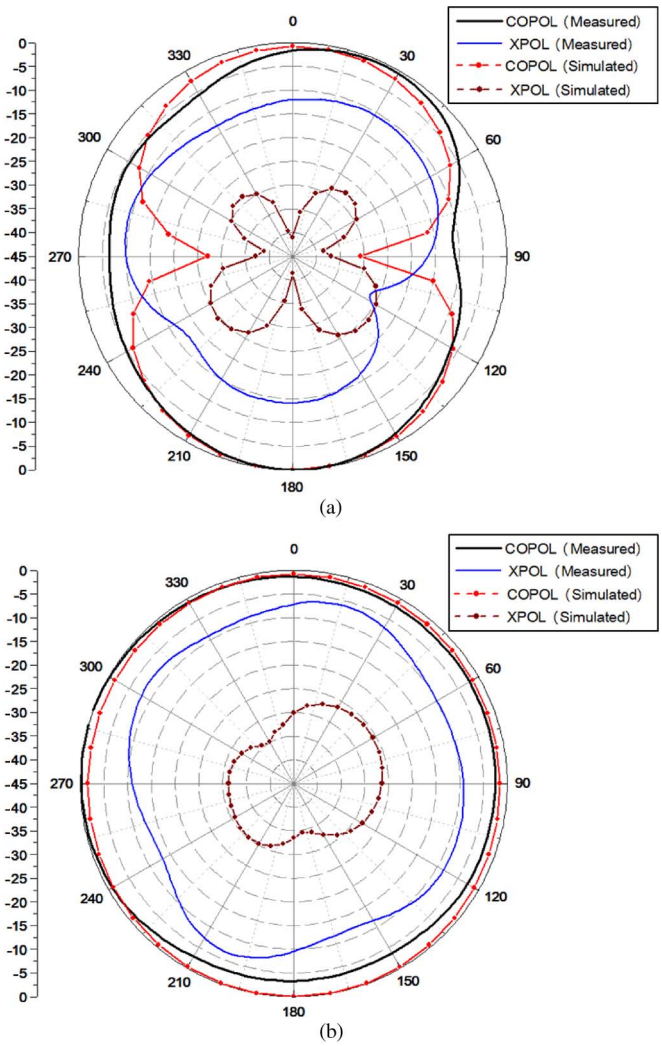

Fig. 13. Simulated and measured radiation patterns of the chip-loaded ZOR antenna at 2.38 GHz (a) y-z plane (E-plane), (b) x-z plane (H-plane).

TABLE II
MEASUREMENT SUMMARY AND COMPARISON RESULTS FOR THREE PROPOSED ANTENNAS

	Symmetric	Asymmetric	Chip-Loaded
Frequency (GHz)	2.03	1.5	2.38
Size (λ_0)	0.097 × 0.053 × 0.011	0.072 × 0.04 × 0.008	0.128 × 0.07 × 0.012
Bandwidth (%)	6.8	4.8	8.9
Gain (dBi)	1.35	-2.15	1.54
Efficiency (%)	62	42.5	77.8

V. SUMMARY AND COMPARISON

The overall antenna performances of the three proposed antennas are compared in Table II. Their overall physical sizes are identical, except that the shorted meander lines of the unit cell are differently designed. In other words, the values of L_R, C_L, and C_R in two of the models are the same and only the value of L_L is varied.

The asymmetric antenna is designed by removing one side of the meander line of the unit cells from the symmetric antenna. Since the L_L of the asymmetric antenna is higher than that of the symmetric antenna, its resonant frequency is decreased from 2.03 GHz to 1.5 GHz. Therefore, its electrical size can be further reduced in the asymmetric geometry. As a trade-off, the radiation efficiency is degraded due to the electrically smaller aperture size of the asymmetric antenna. Furthermore, the coupled slot mode originating from the discontinuity of the asymmetric antenna affects its radiation efficiency. The measured efficiencies of the symmetric and asymmetric antennas are 62% and 42.5%, respectively. In addition, their measured peak gains are 1.35 dBi and −2.15 dBi, respectively.

The chip-loaded antenna is designed by replacing the meander lines by chip inductors. Since the chip inductance is easily adjustable, it has the advantage of easy realization at the desired frequency. However, the value of the chip inductance is not acceptable at high frequencies. The chip-loaded antenna shows the highest efficiency of 77.8% and its peak gain is 1.54 dBi at 2.38 GHz. The radiation efficiencies are obtained by measuring the total radiation power versus the input power.

The symmetric, asymmetric, and chip-loaded antennas provide extended 10 dB bandwidths of 6.8%, 5%, and 8.9%, respectively. Although the asymmetric antenna has a higher L_L, its bandwidth is decreased. This is because the balancing of Y'_{shunt} is not achieved and G is decreased.

In terms of the radiation mechanisms of the proposed antenna, the magnitudes of the magnetic current densities in each patch edge are not equivalent. The dominant magnetic current source is from one slot which is located at the feeding line. The magnetic current sources from the other three slots are weaker because the signal plane is far from the ground plane. Therefore, the proposed antenna looks like an ideal magnetic dipole rather than the magnetic loop antenna described in [10].

At the zeroth-order resonant frequency, the resonant condition is independent of the aperture dimension. Fig. 14(a) clearly demonstrates that the resonant frequencies remain almost constant as the aperture dimension is increased. In a conventional resonant antenna, it is obvious that the resonant frequency is decreased as its size is increased. Fig. 14(b) shows the relationship between the gain and the number of unit cells. As shown in Fig. 14(a) and (b), the frequencies of these antennas do not vary much while their gains become higher as the number of the unit cells increases.

Furthermore, the measured radiation patterns show that the cross-polarization levels of the proposed antennas are higher than the simulated ones. These differences are due to the fabrication limitation resulting from the fine meander lines and the measurement error resulting from the much smaller size of the aperture compared with that of the RF cable in the test environment.

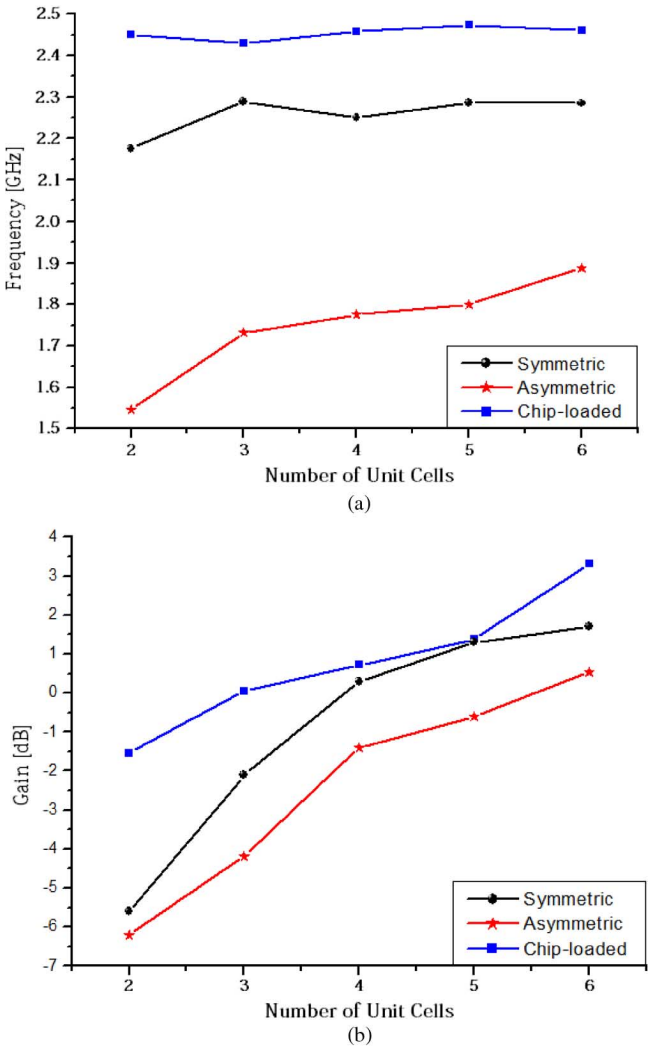

Fig. 14. Comparison of the symmetric, asymmetric, and chip-loaded antennas (a) relationship between the frequency and the number of unit cells and (b) relationship between the gain and the number of unit cells.

VI. Conclusion

In this study, we demonstrated the extended bandwidth of the proposed CPW-fed ZOR antennas. The size of the proposed ZOR antennas can be reduced, due to their zeroth-order resonance. When the ZOR antennas are realized using CPW technology, they allow for the design freedom of the shunt parameters in the equivalent circuit model. Thus, when a high shunt inductance and small shunt capacitance are realized, the symmetric and asymmetric ZOR antennas exhibit extended bandwidths of 6.8% and 5%, respectively.

Alternatively, when chip inductors are applied to the proposed CPW ZOR antenna, its bandwidth can be improved by up to 8.9%. In order to analyze the principle of this bandwidth enhancement, the equivalent-circuit models were derived and analyzed. The proposed theory and experimental results show good agreement with each other. In addition, the proposed design has the advantages of easy fabrication, due to the via free structure, as well as a single layer process. Therefore, due to their features, the symmetric, asymmetric, and chip-loaded antennas are suitable for use in mobile wireless communication systems.

References

[1] V. G. Veselago, "The electrodynamics of substances with simultaneously negative values of ε and μ," *Sov. Phys. Usp*, vol. 10, no. 4, pp. 509–514, Jan.–Feb. 1968.

[2] G. V. Eleftheriades, A. K. Iyer, and P. C. Kremer, "Planar negative refractive index media using periodically LC loaded transmission lines," *IEEE Trans. Microw. Theory Tech.*, vol. 50, no. 12, pp. 2702–2712, Dec. 2002.

[3] G. V. Eleftheriades, A. Grbic, and M. Antoniades, "Negative-refractive-index metamaterials and enabling electromagnetic applications," in *Proc. IEEE Int. Symp. Antennas and Propag.*, Monterey, CA, Jun. 2004, vol. 2, pp. 1399–1402.

[4] G. V. Eleftheriades, "Enabling RF/microwave devices using negative-refractive-index transmission-line (NRI-TL) metamaterials," *IEEE Antennas Propag. Mag.*, vol. 49, no. 2, pp. 34–51, Apr. 2007.

[5] G. V. Eleftheriades, M. A. Antoniades, and F. Qureshi, "Antenna applications of negative-refractive index transmission-line structures," *IET Microw., Antennas Propag.*, vol. 1, no. 1, pp. 12–22, Feb. 2007.

[6] A. Lai, T. Itoh, and C. Caloz, "Composite right/left-handed transmission line metamaterials," *IEEE Microw. Mag.*, vol. 5, no. 3, pp. 34–50, Sep. 2004.

[7] S. Lim, C. Caloz, and T. Itoh, "Metamaterial-based electronically controlled transmission-line structure as a novel leaky-wave antenna with tunable radiation angle and beamwidth," *IEEE Trans. Microw. Theory Tech.*, vol. 53, pp. 161–173, Jan. 2005.

[8] A. Sanada, C. Caloz, and T. Itoh, "Novel zeroth-order resonance in composite right/left-handed transmission line resonators," in *Proc. Asia-Pacific Microwave Conf.*, Seoul, Korea, Nov. 2003, vol. 3, pp. 1588–1592.

[9] C.-J. Lee, K. M. K. H. Leong, and T. Itoh, "Composite right/left-handed transmission line based compact resonant antennas for RF module integration," *IEEE Trans. Antennas Propag.*, vol. 54, pp. 2283–2291, Aug. 2006.

[10] A. Lai, K. M. K. H. Leong, and T. Itoh, "Infinite wavelength resonant antennas with monopole radiation pattern based on periodic structures," *IEEE Trans. Antennas Propag.*, vol. 55, no. 3, pp. 868–875, Mar. 2007.

[11] F. Qureshi, M. A. Antoniades, and G. V. Eleftheriades, "A compact and low-profile metamaterial ring antenna with vertical polarization," *IEEE Antenna Wireless Propag. Lett.*, vol. 4, pp. 333–336, 2005.

[12] C.-J. Lee, K. M. K. H. Leong, and T. Itoh, Broadband Small Antenna for Potable Wireless Application *iWat*, pp. 10–13, Mar. 2008.

[13] J. Zhu and G. V. Eleftheriades, "A compact transmission line metamaterial antenna with extended bandwidth," *IEEE Antenna Wireless Propag. Lett.*, vol. 8, pp. 295–298, 2009.

[14] M. A. Antoniades and G. V. Eleftheriades, "A broadband dual-mode monopole antenna using NRI-TL metamaterial loading," *IEEE Antenna Wireless Propag. Lett.*, vol. 8, pp. 258–261, 2009.

[15] T. Jang and S. Lim, "A novel broadband co-planar waveguide (CPW) zeroth order resonant antenna," in *Proc. Asia-Pacific Microwave Conf.*, Singapore, Dec. 2009, pp. 52–55.

[16] A. Sanada, C. Caloz, and T. Itoh, "Planar distributed structures with negative refractive index," *IEEE Trans. Microw. Theory Tech.*, vol. 52, no. 4, pp. 1252–1263, Apr. 2004.

[17] D. M. Pozar, *Microwave Engineering*, 2nd ed. Toronto: Wiley, 1998, pp. 49–57.

[18] R. L. Fante, "Quality factor of general ideal antennas," *IEEE Trans. Antennas Propag.*, vol. 17, no. 2, pp. 151–155, Mar. 1969.

[19] A. D. Yaghjian and S. R. Best, "Impedance, bandwidth, and Q of antennas," *IEEE Trans. Antennas Propag.*, vol. 53, p. 1298, 2005.

[20] C. Caloz and T. Itoh, *Electromagnetic Metamaterials: Transmission Line Theory and Microwave Applications*. New York: Wiley, Dec. 2005.

[21] G. V. Eleftheriades and K. G. Balmain, *Negative-Refraction Metamaterials: Fundamental Principles and Applications*. New York: Wiley/IEEE Press, Jun. 2005.

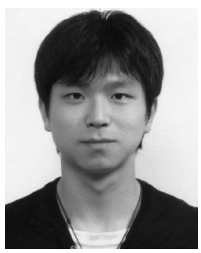

Taehee Jang (S'09) received the B.S. degree in the school of electrical and electronics engineering from the Chung-Ang University, Seoul, Korea, in 2009.

Since 2008, he has been worked as a Student Researcher in the Microwave Wireless Communication Laboratory, Chung-Ang University, Seoul, Korea. His research interests include metamaterial applications and printed antennas.

Jaehyurk Choi received the B.S. degree in the school of electrical and electronics engineering from the Chung-Ang University, Seoul, in 2009, where he is currently working toward the M.S. degree in electrical and electronics engineering.

His research interests include metamaterial applications and reconfigurable antennas.

Sungjoon Lim (S'02–M'07) received the B.S. degree in electronic engineering from Yonsei University, Seoul, Korea, in 2002, and the M.S. and Ph.D. degrees in electrical engineering from the University of California at Los Angeles (UCLA), in 2004 and 2006, respectively.

After a postdoctoral position at the Integrated Nanosystem Research Facility (INRF), the University of California at Irvine, he joined the School of Electrical and Electronics Engineering, Chung-Ang University, Seoul, Korea, in 2007, where he is currently an Assistant Professor. He has authored and coauthored more than 30 technical conference, letter and journal papers. His research interests include engineered metamaterial structures, printed antennas, arrays, and RF MEMS applications. He is also interested in the modeling and design of microwave/millimeter-wave circuits.

Dr. Lim received the Institution of Engineering and Technology (IET) Premium Award in 2009.